Spontaneous Transfer of Ganglioside GM_1 from Its Micelles to Lipid Vesicles of Differing Size†

Rhoderick E. Brown* and Kristi J. Hyland

The Hormel Institute, University of Minnesota, Austin, Minnesota 55912

Received January 21, 1992; Revised Manuscript Received August 13, 1992

ABSTRACT: The spontaneous incorporation of II^3-*N*-acetylneuraminosylgangliotetraosylceramide (GM_1) from its micelles into phospholipid bilayer vesicles has been investigated to determine whether curvature-induced changes in membrane lipid packing influence ganglioside uptake. Use of conventional liquid chromatography in conjunction with technically-improved molecular sieve gels permits ganglioside micelles to be separated from phospholipid vesicles of different average size including vesicles with diameters smaller than 40 nm and, thus, allows detailed study of native ganglioside GM_1 incorporation into model membranes under conditions where complicating processes like fusion are readily detected if present. At 45 °C, the spontaneous transfer rate of GM_1 from its micelles to small unilamellar vesicles (SUVs) comprised of 1-palmitoyl-2-oleoyl-*sn*-glycero-3-phosphocholine (POPC) is at least 3-fold faster than that to similar composition large unilamellar vesicles (LUVs) prepared by octyl glucoside dialysis. Careful analysis of ganglioside GM_1 distribution among vesicle populations of differing average size reveals that GM_1 preferentially incorporates into the smaller vesicles of certain populations. This behavior is observed in SUVs as well as in LUV–SUV mixtures and actually serves as a sensitive indicator for the presence of trace quantities of SUVs in various LUV preparations. Analysis of the results shows that both differences in the diffusional collision frequency between GM_1 monomers and either SUVs or LUVs and curvature-induced changes in the interfacial lipid packing in either SUVs or LUVs can dramatically influence spontaneous ganglioside uptake. The results have important implications for physiological studies involving sphingolipid-mediated cell signaling events as well as diagnostic paradigms of lysosomal sphingolipid storage diseases in which radiolabeled or fluorescent gangliosides are incorporated into cultured cells by coincubation.

Gangliosides are participants in many important events occurring at the cell surface including the binding of various antibodies, pericellular adhesive proteins, bacterial toxins, and viruses to the plasma membrane [for reviews, see Curatolo (1987b) and Karlsson (1989)]. These sialylated sphingolipids have been also been implicated in the regulation of protein kinase C, in nerve regeneration, and in other metabolic processes involving cellular differentiation, growth, and development (Hannun & Bell, 1989; Ledeen, 1984; Hakomori, 1990).

Ganglioside involvement in cellular events was recognized because, when they are incubated with cultured cells, these glycolipids rapidly and spontaneously incorporate themselves into plasma membranes [for review, see Brown (1990)]. Such behavior is a consequence of the solubility properties of gangliosides in aqueous solution. Compared to most naturally-occurring diacylphospholipids, gangliosides have relatively large polar headgroups. Thus, the hydrophile–lipophile balance among gangliosides usually favors formation of micelles and high monomer concentrations in excess water [for reviews, see Curatolo (1987a), Thompson and Brown (1988), and Corti et al. (1991)].

To date, only a few studies have focused on ganglioside transfer from its micelle to phospholipid vesicles (Felgner et al., 1981, 1983; Masserini & Freire, 1987). From these studies, it is clear that, upon coincubation, gangliosides spontaneously incorporate themselves into phospholipid vesicles. The more polar the ganglioside (e.g., tri- vs monosialoganglioside), the more rapidly it incorporates into the outer monolayers of phospholipid bilayer vesicles with carbohydrate residues projecting into the external environment (Felgner et al., 1981, 1983). At low micelle-to-vesicle ratios, ganglioside transfer is independent of vesicle concentration, suggesting that transfer occurs primarily by diffusion of ganglioside monomers through the aqueous medium rather than by collisional contacts between micelles and phospholipid vesicles. Because the previous studies were performed with large unilamellar vesicles (LUVs),[1] it is not clear whether curvature-induced changes in membrane lipid packing can regulate ganglioside uptake. Understanding such processes is important for interpreting physiological studies involving sphingolipid-mediated cell signaling events as well as diagnostic paradigms of lysosomal sphingolipid storage diseases in which radiolabeled or fluorescent gangliosides are incorporated into cultured cells by coincubation.

In the present investigation, we have studied the spontaneous transfer of radiolabeled ganglioside GM_1 from its micelles to lipid vesicles of different avearage size using conventional molecular sieve liquid chromatography. This approach has permitted detailed study of native ganglioside GM_1 incorporation into model membranes under conditions where complicating processes like fusion are readily detected if present. The results show that curvature-induced changes in the interfacial lipid packing within bilayer vesicles dramatically influence spontaneous ganglioside uptake. A preliminary

† This research was supported by USPHS Grant GM45928 and the Hormel Foundation.

* To whom correspondence should be addressed.

[1] Abbreviations: GM_1, II^3-*N*-acetylneuraminosylgangliotetraosylceramide; POPC, 1-palmitoyl-2-oleoyl-*sn*-glycero-3-phosphocholine; LPC, 1-palmitoyl-*sn*-glycero-3-phosphocholine; SUV(s), small unilamellar vesicle(s); LUV(s), large unilamellar vesicle(s); OG, octyl glucoside; DMPC, dimyristoyl-*sn*-glycero-3-phosphocholine; PC, phosphatidylcholine; DPPC, dipalmitoyl-*sn*-glycero-3-phosphocholine.

0006-2960/92/0431-10602$03.00/0

report of portions of this work has appeared elsewhere (Brown & Hyland, 1992).

MATERIALS AND METHODS

Vesicle Preparation and Size Analysis. Small unilamellar vesicles (SUVs), comprised of 1-palmitoyl-2-oleoyl-*sn*-glycero-3-phosphocholine (POPC) (Avanti Polar Lipids, Alabaster, AL), were prepared by sonication (Barenholz et al., 1977). Large unilamellar POPC vesicles (LUVs) were prepared either by octyl glucoside (OG) dialysis (Jackson et al., 1982) or by extrusion using filters with either 100-nm- or 200-nm-diameter pores (Mayer et al., 1986). SUVs comprised of 25 mol % 1-palmitoyl-*sn*-glycero-3-phosphocholine (LPC) in POPC were prepared as described by Kumar et al. (1989). Vesicle concentrations were determined by lipid phosphate assays (Rouser et al., 1970).

The size distributions of the LUV preparations were assessed by freeze-fracture electron microscopy. Small aliquots of lipid vesicle preparations were placed on gold alloy specimen carriers and frozen in liquid Freon 22 cooled by liquid nitrogen. Replicas were produced by fracturing specimens at −110 °C in a Balzers BAF300 freeze-fracture apparatus equipped with an electron gun for Pt/C shadowcasting (45° angle) and a resistance evaporator for depositing carbon support films. Replicas were floated onto distilled water, picked up on untreated 300-mesh copper grids, and cleaned with $CHCl_3$/CH_3OH (2:1) to remove residual lipid before being examined in a JEOL S-100 electron microscope. Accurate measurements of vesicle diameters were obtained from resulting micrographs (total magnification 56000×) by including only equatorially-fractured vesicles in the size distribution analysis. An equatorially fractured vesicle displays exactly 50% coverage with Pt/C at a shadowing angle of 45° when the fracture plane through the vesicle is concave (van Venetie et al., 1980).

Ganglioside Preparation and Characterization. Mixed gangliosides (di- and trisialogangliosides) were obtained from the upper Folch extract of bovine brains (Avanti Polar Lipids, Alabaster, AL) using molecular sieve and ion-exchange chromatography (Brown et al., 1985) and were treated with neuraminidase to produce ganglioside GM_1 (Brown & Thompson, 1987). Following isolation by silicic acid chromatography (Felgner et al., 1983), GM_1 purity was checked by thin-layer chromatography [$CHCl_3$/CH_3OH/0.02% aqueous $CaCl_2$, 55:45:10, or acetonitrile/2-propanol/50 mM aqueous KCl, 10:67:23] (Ando et al., 1987) using primulin, orcinol, and resorcinol for detection (Kundu, 1981). GM_1 concentration in stock solutions was determined both by dry weight and by chemical determination of nitrogen content (Sloan-Stanley, 1967).

GM_1 fatty acyl chain composition was analyzed by gas chromatography on an OV-17 column (160–220 °C, 3 °C/min, detector at 250 °C). Prior to analysis, fatty acids were released by heating GM_1 for 18 h at 70 °C in 1 N methanolic HCl (CH_3OH/H_2O, 82:18 v/v) (Naoi et al., 1974) and were methylated with diazomethane (Schlenk & Gellerman, 1960). The GM_1 acyl composition consisted of $C_{16:0}$ (0.4%), $C_{18:0}$ (92%), $C_{20:0}$ (7.4%), $C_{22:0}$ (0.4%), and miscellaneous components (0.4%). $C_{m:n}$ designates the fatty acyl chain where m is the number of carbon atoms and n is the number of double bonds. Values are reported as weight percent.

Preparation of Tritiated GM_1. Radioactive GM_1 was synthesized as described previously (Brown & Thompson, 1987) but was purified as described below. Briefly, alcohol groups at the sixth carbon of terminal galactose residues were oxidized using galactose oxidase. Resulting aldehyde groups were reduced back to their original carbinol configurations using tritiated sodium borohydride. Labeled GM_1 was recovered by elution through a C-18 reverse-phase cartridge (Williams & McCluer, 1980) and repurified by HPLC using a 10-μm silicic acid column (10 × 25 mm; Alltech) at a flow rate of 2 mL/min. After loading, the column was washed for 1 min with a solvent mixture consisting of hexane/2-propanol/water (HIW) (55:42:3) and 10% HIW (55:27:14.6). Over the next 30 min, the content of HIW (55:27:14.6) was increased linearly until it reached 40% and was then held constant for an additional 10 min. Eluted GM_1, detected at 214 nm and by liquid scintillation counting, was over 98% pure.

Molecular Sieve Chromatography. Incubations were performed in gastight glass syringes such that no air bubbles were present and in 20 mM Na-PIPES buffer (pH 7.0) containing 0.02% sodium azide along with a 5-fold molar excess of EDTA relative to ganglioside GM_1 to avoid complications due to micelle or vesicle fusion. Unless stated otherwise, the mole fraction of ganglioside GM_1 was 2.5 with respect to total lipid at the start of each incubation. At this mole fraction, ganglioside GM_1 is eventually completely incorporated into the phospholipid vesicles (Felgner et al., 1983). At designated times, phospholipid vesicles of differing size were separated by elution through either a Sephacryl S-500 or a Sephacryl S-1000 column (40 × 1 cm) at room temperature while employing an upward hydrostatic pressure of 55 cm. Separation of phospholipid vesicles and GM_1 micelles was achieved under similar conditions but using Sephacryl S-300 and required about 75 min. Columns were prepared and used as described previously (Brown et al., 1985; Brown & Thompson, 1987). Vesicle recovery was generally between 80% and 95% based on lipid phosphate.

Analysis of GM_1 Transfer Data. Transfer was quantitated by integrating the [^{3}H]-GM_1 that coeluted with the phosphate profile of the POPC vesicles and comparing the [^{3}H]-GM_1/phosphate ratio in the original incubation mixture with the ratio obtained in the recovered vesicle fractions. Data was analyzed similarly to the method described by Brown and Thompson (1987). When analyzed as a reversible pseudo-first-order kinetic process, the following expression was used:

$$\frac{X(t) - X(\infty)}{X(0) - X(\infty)} = \exp(-kt)$$

where $X(t)$ is the [^{3}H]-GM_1 fractional transfer from the micelles at time t, $X(0)$ is the total amount of [^{3}H]-GM_1 present in the micelles at time zero, $X(\infty)$ is the calculated equilibrium value for the [^{3}H]-GM_1 fractional transfer from the micelles at infinite time, and k is the rate constant for departure from the micelles. In theory, $X(\infty)$ should be 1 for GM_1 micelles (Felgner et al., 1983; Masserini & Freire, 1987). However, because separation of micelles and vesicles is not complete, $X(\infty)$ must be determined empirically for given column conditions and for each vesicle preparation. In these studies, $X(\infty)$ equals 0.95 for POPC SUVs, 0.97 for POPC OG-dialysis LUVs, and 0.88 for POPC/LPC SUVs.

Kinetic parameters were determined by applying an iterative nonlinear least-squares analysis (Enzfitter, Elsevier-BIOSOFT). The best fit was determined after evaluating the data using one-exponential or the sum of two-exponential functions with or without a constant equilibrium value on a Gateway 2000 486/33C computer.

The GM_1 incorporation index shown as insets in Figures 1, 3, 4, and 6 provides a relative measure of the deviation from ideality of GM_1 incorporation among a given vesicle population. This index is the difference between the observed and

random GM_1 distribution among vesicle fractions weighted for the relative amount of lipid phosphate in each fraction. The random GM_1 distribution is simply the GM_1 mole percent expected in each fraction if the incorporation occurs with equal efficacy among all vesicles in the population and is identical to the total GM_1 mole percent in the incubation mix. The observed GM_1 distribution is calculated by comparing the GM_1/lipid phosphate ratio in the starting incubation mix with the GM_1/lipid phosphate ratio measured in each eluted fraction containing vesicles. If no difference exists between the observed and the random GM_1 distributions, the GM_1 incorporation index is zero. If the observed GM_1 distribution exceeds the random distribution, a positive incorporation index results. This indicates that the mole fraction of GM_1 in the vesicles is higher than would be expected by simple dilution among all vesicles. Conversely, if the random GM_1 distribution exceeds the observed distribution, a negative incorporation index results. This indicates that the GM_1 mole fraction in the vesicles is lower than would be expected by dilution among all vesicles. The incorporation index is reproducible and constant for a given phospholipid vesicle preparation at a given phospholipid/ganglioside ratio and under constant experimental conditions (temperature, pH, ionic strength, etc.). However, as is shown under Results, the incorporation index does change as the heterogeneity of a vesicle population increases and does depend on how much of certain-sized vesicles are present.

RESULTS

Resolution of Micelles and Vesicles. Prior to determination of whether spontaneous ganglioside incorporation into phospholipid vesicles is influenced by vesicle size, experimental conditions were established for resolving ganglioside micelles and phospholipid vesicles of various sizes. Previously, Felgner et al. (1981) reported that ganglioside micelles and phospholipid vesicles could be separated by molecular sieve chromatography if the vesicles were large (e.g., 70-nm diameter), but not when the vesicles were small (e.g., 25-nm diameter). Also, Harris and Thornton (1978) were unable to resolve a mixture of egg phosphatidylcholine (PC) small unilamellar vesicles (SUVs) and ganglioside micelles using Sepharose 4B chromatography. Figure 1A shows that successful resolution of PC SUVs and ganglioside GM_1 micelles can be achieved by molecular sieve chromatography using Sephacryl S-300. SUVs (approximately 2×10^6 Da) elute near the column's void volume, whereas ganglioside GM_1 micelles (approximately 0.4×10^6 Da) elute within the column's included volume. There was no change in the elution position of PC vesicles or GM_1 micelles if they were incubated separately at 47 °C for time intervals between 0 and 18 h (data not shown). In other control experiments, larger vesicles also eluted at the column's void volume (data not shown). In general, the higher rigidity of Sephacryl gels permits resolution at faster flow rates compared to agarose-based gels, along with improved molecular weight fractionation range for lipid vesicles and micelles (Brown & Thompson, 1987).

Ganglioside Incorporation into POPC Vesicles. To test whether phospholipid vesicle size affects the spontaneous incorporation of ganglioside GM_1, POPC vesicles of different diameters were incubated with GM_1 micelles at 45 °C for varying time periods. The GM_1 concentration was either 2.5 or 5 mol % with respect to PC. Such conditions promote micelle disappearance as the ganglioside intercalates into the outer leaflets of the bilayer vesicles (Felgner et al., 1981). Moreover, the transfer mechanism, as determined by rapid

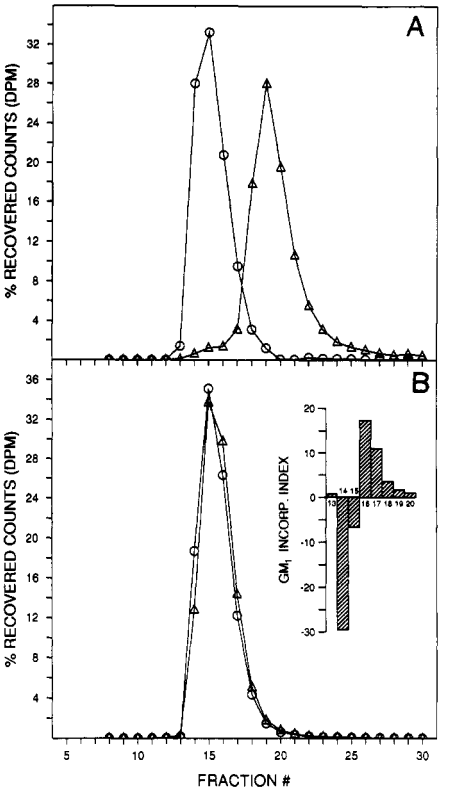

FIGURE 1: Separation of POPC SUVs and GM_1 micelles. (A) (○) Normalized lipid phosphate and (△) [^{3}H]-GM_1 dpm profiles. POPC SUVs (7.5 μmol) and GM_1 micelles (0.38 μmol; 30 000 cpm) were mixed together at room temperature in 0.5 mL of buffer and immediately fractionated on a Sephacryl S-300 column (0.8 × 40 cm). Each eluted fraction contained 0.96 mL. Buffer consists of 20 mM Na-PIPES (pH 7.0) containing 1.0 mM EDTA and 0.02% sodium azide. (B) Same as panel A except that SUVs and GM_1 were incubated together for 6 h at 47 °C prior to fractionation on the Sephacryl S-300 column. Calculation of the GM_1 incorporation index is described under Materials and Methods.

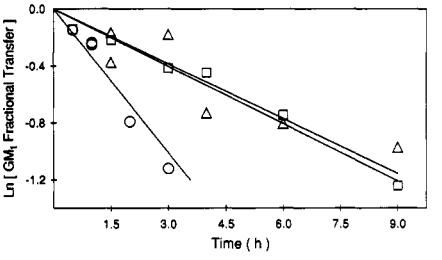

FIGURE 2: Natural logarithm of the GM_1 mole fraction incorporated into phospholipid vesicles as a function of time. [^{3}H]-GM_1 micelles (2.5 mol %) and phospholipid vesicles were separated using the Sephacryl S-300 column described in Figure 1 after incubation for the indicated time at 45 °C. [^{3}H]-GM_1 incorporation into POPC SUVs (○), into POPC OG-dialysis LUVs (□), and into LPC–POPC (25:75) SUVs (△) is shown. Average vesicle radii are indicated in Table I.

separation or fluorescence techniques, involves ganglioside monomers diffusing through the aqueous medium to the PC vesicles (Felgner et al., 1983; Masserini & Freire, 1987). Figure 2 shows a logarithmic plot of GM_1 incorporation into vesicles of different average size or composition. Calculation of the initial rate constants and half-times of spontaneous incorporation (Table I) reveals that GM_1 uptake into POPC SUVs is nearly 3-fold faster than with POPC LUVs prepared by octyl glucoside dialysis. These kinetic data and resulting parameters (e.g., Figure 2 and Table I) should be treated as approximations. The required separation time to fractionate vesicles and ganglioside micelles precludes the possibility of obtaining high-precision data in the early time regime (<1 h).

Table I: GM_1 Transfer Rate Parameters[a]

vesicle	composition	k^b (h^{-1})	$t_{1/2}{}^b$ (h)
SUV	POPC	0.326 ± 0.033	2.13
LUV	POPC	0.131 ± 0.008	5.28
SUV	POPC–LPC (3:1)	0.112 ± 0.018	6.18

[a] Calculated as described under Materials and Methods. [b] Incubation temperature was 45 °C. Vesicle radii for POPC SUVs averaged 15 ± 2 nm, for POPC OG-dialysis LUVs averaged 185 ± 40 nm, and for POPC–LPC SUVs averaged 13 ± 2 nm. For other details, refer to Figure 2 legend.

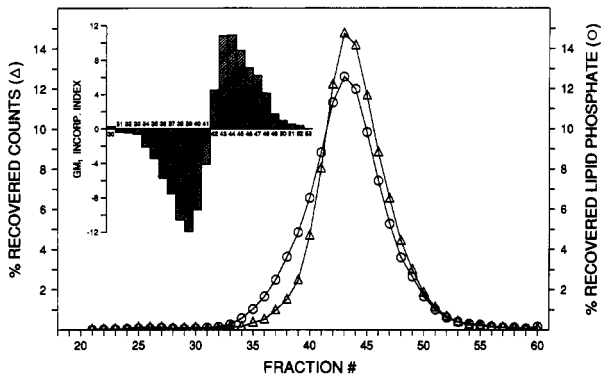

FIGURE 3: Fractionation of POPC SUVs containing incorporated GM_1. (○) Normalized lipid phosphate and (△) [^{3}H]-GM_1 dpm profiles. Fractions 13–21 shown in Figure 1B were pooled, concentrated by ultrafiltration (0.63 mL), and fractionated on a Sephacryl S-500 column (0.8 × 42 cm). Each eluted fraction contained 0.96 mL.

Nevertheless, during the experiments with POPC SUVs and GM_1 micelles, an interesting pattern emerged in the molecular sieve elution profiles. After incubation for time periods sufficient for GM_1 to incorporate into the vesicles, the GM_1 and POPC elution profiles, although very similar, do not superimpose. In fact, the GM_1 profile is shifted slightly toward the trailing fractions of the POPC SUV profile at an elution position that is different from that of GM_1 micelles (Figure 1B). This is clearly illustrated in the inset of Figure 1B, which shows the relative GM_1 depletion in the early-eluting vesicles and the relative GM_1 enrichment in the later-eluting vesicles. This behavior cannot be due to increased micelle size. As pointed out above and by others (Cantu et al., 1986), the average size of ganglioside GM_1 micelles does not change with time when temperature is constant. Thus, if the ganglioside micelles were enlarging to SUV-sized objects, it would have to be due to the transfer of significant amounts of PC into the micelles. However, such transfer has not been observed for liquid-crystalline DPPC (Felgner et al., 1983).

Two other experiments were performed to verify the data in Figure 1B). First, the fractions from the Sephacryl S-300 column corresponding to the POPC vesicles along with coeluting GM_1 were pooled, concentrated by ultrafiltration, and refractionated by molecular sieve chromatography but using Sephacryl S-500. Figure 3 shows clearly that the POPC and GM_1 profiles are not superimposable and that more of the GM_1 elutes with the trailing fractions of the SUV profile. Unlike Sephacryl S-300, in which SUVs are nearly voided, Sephacryl S-500's molecular weight fractionation range is particularly suited for resolving vesicles in this size range (Brown & Thompson, 1987). A second control experiment was performed to determine whether a "lag" occurs in the ganglioside profile if GM_1 is cosolubilized with POPC prior to SUV formation. After cosolubilization, the organic solvent was evaporated and the resulting SUVs eluted as before (e.g., Figure 3), which is consistent with known effects of low GM_1

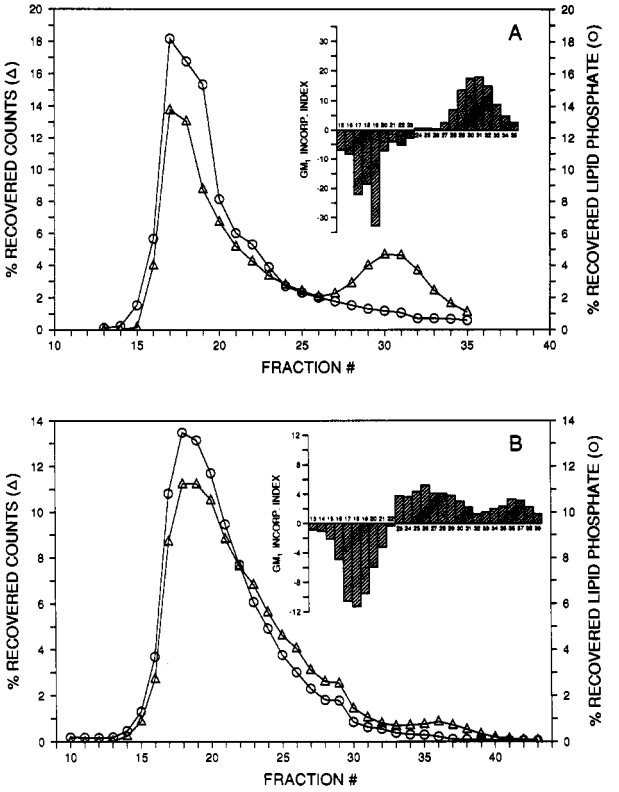

FIGURE 4: Fractionation of POPC LUVs after incubation with ganglioside GM_1 micelles. (○) Normalized lipid phosphate and (△) [^{3}H]-GM_1 dpm profiles. (A) POPC OG-dialysis LUVs (7.5 μmol) and GM_1 micelles (0.38 μmol; 40 000 cpm) were mixed together in 0.5 mL of buffer, incubated for 18 h at 45 °C, and then fractionated on a Sephacryl S-1000 column (1 × 40 cm). Each eluted fraction contained 0.925 mL. (B) POPC extrusion LUVs (7.5 μmol) prepared with the 100-nm pore filter and GM_1 micelles (0.38 μmol; 60 000 cpm) were mixed together in 0.5 mL of buffer, incubated for 22 h at 45 °C, and then fractionated on a Sephacryl S-500 column (1 × 42 cm). Each eluted fraction contained 1.0 mL. A trace of [^{3}H]-GM_1 micelles can be seen in fractions 34–38.

concentrations on vesicle size (Corti et al., 1991). More importantly, there was no lag in the GM_1 profile. Taken together, these results indicate that when GM_1 micelles are incubated with POPC SUVs, GM_1 preferentially incorporates itself into the smaller vesicles of the population.

To estimate the average radii of the POPC SUV population, quasi-elastic light scattering (QELS) analysis was performed. Measurements made at 90° and analyzed by the method of cumulants revealed an average radius of 15 ± 2 nm. On the basis of these determinations, the vesicles preferred by GM_1 (Figure 3) would have radii equal to or less than 15 nm.

To determine whether GM_1's preference for the smaller vesicles of a population is limited to SUVs, experiments were performed with various POPC LUV preparations. We incubated GM_1 for 18 h at 45 °C with LUVs prepared by OG-dialysis and fractionated using Sephacryl S-1000 (Figure 4) because this gel possesses a pore size large enough to fractionate vesicles with radii up to 130 nm (Nozaki et al., 1982; Reynolds et al., 1983). As shown in Figure 4, most of the [^{3}H]-GM_1 coelutes with the PC peak eluting near the void volume. However, a smaller but clearly resolved GM_1 peak also elutes along the trailing edge of the phosphate peak. This second peak, which contains 16.5% of the total [^{3}H]-GM_1, but very little lipid phosphate, corresponds to the elution position of POPC SUVs in the 22–45-nm diameter size range.

It is important to note that SUVs containing GM_1 cannot account for a significant portion of the ^{3}H peak near the void

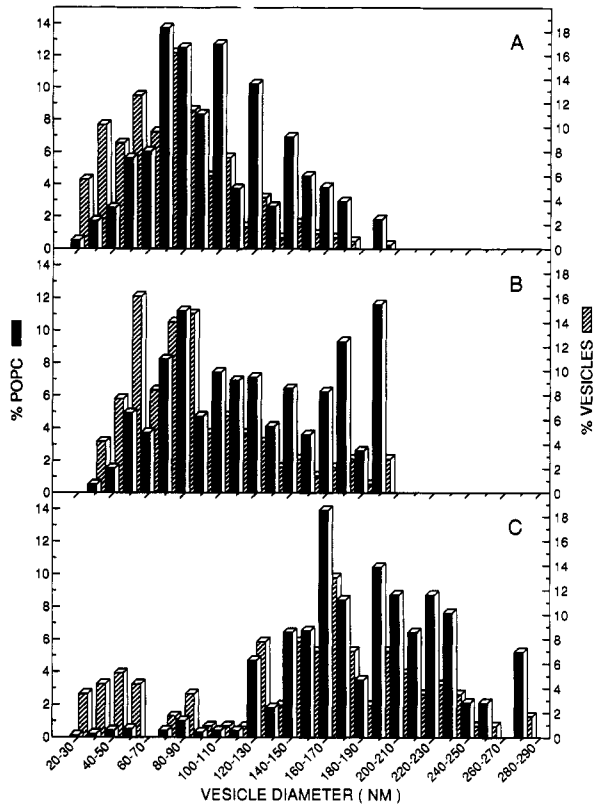

FIGURE 5: Freeze-fracture electron microscopic analysis of different phospholipid vesicle preparations. POPC extrusion vesicles prepared with (A) 100-nm- or (B) 200-nm-diameter filters; (C) POPC LUVs prepared by octyl glucoside dialysis. Size distributions were made by measuring only equatorially concave fractured vesicles (van Venetie et al., 1980) and counting 330 of the 100-nm extrusion vesicles, 145 of the 200-nm extrusion vesicles, and 115 of the OG-dialysis vesicles. Details of vesicle preparation and freeze-fracture electron microscopy are provided under Materials and Methods. The solid bars represent the mass-weighted diameter distributions calculated from the number-weighted distributions (hatched bars) using the assumptions of Chapman et al. (1990).

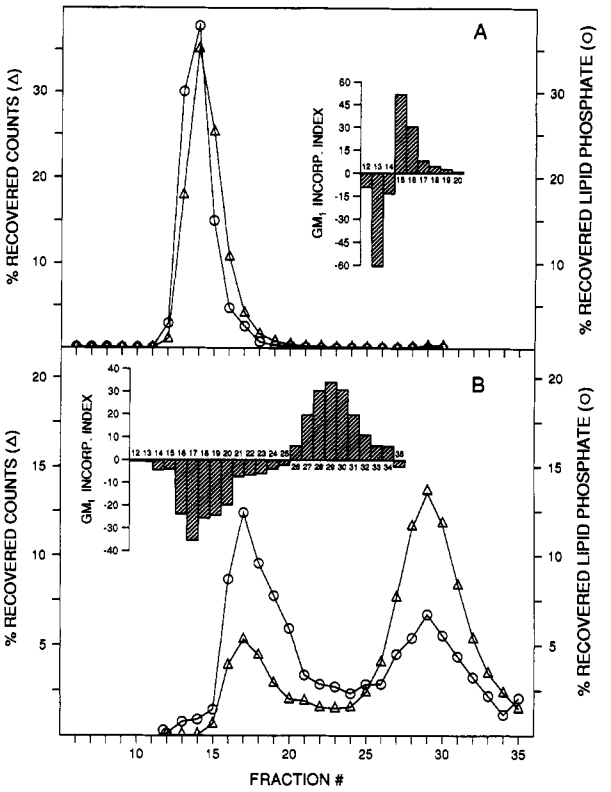

FIGURE 6: Fractionation of POPC OG-dialysis LUVs and SUVs after GM_1 incorporation. (O) Normalized lipid phosphate and (Δ) [^{3}H]-GM_1 dpm profiles. POPC OG-dialysis LUVs (4.88 μmol), POPC SUVs (2.62 μmol), and GM_1 micelles (0.38 μmol; 36 000 cpm) were mixed together in 0.5 mL of buffer, incubated for 18 h at 45 °C, and then (A) half the mixture was fractionated on a Sephacryl S-300 column (1 × 40 cm) and (B) the remaining half was fractionated on a Sephacryl S-1000 column (1 × 40 cm). Each eluted fraction contained 0.94 mL.

volume because of the known resolving capabilities of Sephacryl S-1000 determined by Tanford and colleagues (Nozaki et al., 1982; Reynolds et al., 1983). Moreover, to avoid stable associations and/or fusion between LUVs and SUVs, all experiments were performed at temperatures well above the gel-to-liquid crystalline transition temperature of the phospholipid and in the presence of EDTA [e.g., Lichtenberg and Barenholz (1988)].

In other experiments, LUVs prepared by extrusion rather than OG-dialysis were incubated with GM_1 and fractionated using Sephacryl S-500 (Figure 4B). In prior control experiments, POPC SUVs with average radii of 15 ± 2 nm eluted in fractions 25–34 with peak fractions being 28 and 29 (data not shown). Fractionation of the POPC extrusion vesicles with incorporated GM_1 revealed a broad phosphate profile with a distinct shoulder in fractions 28 and 29. Moreover, a definite lag can be seen in the GM_1 elution profile to the fractions containing the later-eluting SUV-sized vesicles. Because of these results, each of the LUV preparations was carefully examined by freeze-fracture electron microscopy (van Venetie et al., 1980). Figure 5 shows that the vesicles produced by OG-dialysis are generally larger than the extrusion vesicles produced with either 100- or 200-nm filters. More importantly, the size distributions of all three preparations clearly show small, but measurable, quantities of vesicles with average diameters of 45 nm or less. This finding is important because vesicles with small diameters exhibit unusual physical properties, many of which are due to their extreme surface curvature [e.g., Lichtenberg et al. (1981)].

To examine the relationship between vesicle size and ganglioside uptake in more detail, mixtures of LUVs and SUVs were incubated with GM_1 micelles. Then, half the sample was fractionated using a Sephacryl S-300 column in order to confirm that ganglioside was incorporated into the vesicles (Figure 6A). Meanwhile, the other half was fractionated using a Sephacryl S-1000 column in order to separate the large and small vesicles (Figure 6B). With the Sephacryl S-300, both the LUVs and SUVs coelute in the column void volume (Figure 6A). The GM_1 profile is also near the column void volume but, again, is slightly shifted toward the later-eluting POPC vesicles. Comparison with Figure 1A clearly shows that there are no GM_1 micelles in the system. Thus, the results in Figure 6B cannot be due to ganglioside micelles remaining in the vesicle mixture. Rather, the distribution reflects GM_1 association with the two vesicle populations. Interestingly, most of the GM_1 (>80%) coelutes with the SUVs rather than with the LUVs. The distinct preference of GM_1 for SUVs cannot be attributed to differences in available outer surface area of the two bilayer vesicle populations because equal outer surface areas (SUV/LUV 1:2 phosphate ratio) are present.

The preference of GM_1 for SUVs compared to LUVs does not reflect the true equilibrium distribution of the ganglioside within the system. GM_1's half-time of spontaneous interbilayer transfer at 45 °C from SUV donor vesicles to LUV acceptor vesicles is about 40 h and increases 2-fold if the SUV donors are made by sonication and then incubated with GM_1

(Brown & Thompson, 1987). Thus, although GM_1 spontaneously transfers from its micelle to both SUVs and LUVs relatively quickly, once incorporated into a vesicle, its ability to redistribute to other vesicles occurs on a much slower time scale.

GM_1 Incorporation into POPC–LPC SUVs. In principle, GM_1's preference for POPC SUVs either could be due to the unusual surface packing properties of these vesicles or could be due to the higher collisional rates expected between GM_1 monomers and SUVs compared to those between GM_1 and LUVs. To distinguish these two possibilities, GM_1 micelles were incubated with SUVs comprised of 25 mol % 1-palmitoyl-*sn*-glycero-3-phosphocholine (lyso-PC; LPC) and 75 mol % POPC and then fractionated on a Sephacryl S-300 column. Kumar et al. (1989) have shown that the size of POPC–LPC SUVs is nearly identical to that of POPC SUVs but that the lipid headgroup motion, as measured by NMR spin relaxation techniques (T_2*), is slower in the outer monolayers of POPC–LPC SUVs than in POPC SUVs. This indicates that the outer monolayers of POPC–LPC SUVs are packed tighter than those of POPC SUVs. This optimal packing arrangement is highly dependent on the POPC/LPC molar ratio in the SUVs. However, because the POPC–LPC SUVs are similar in size to POPC SUVs, their diffusional rates and hence their collisional rates with GM_1 monomers should be similar.

Incubation of GM_1 micelles with the POPC-LPC SUVs for varying time periods followed by separation on Sephacryl S-300 reveals that the rate of GM_1 uptake is markedly diminished compared to that of POPC SUVs (Figure 2, Table I). Also, the elution profiles of the vesicles and the GM_1 are superimposable with little evidence of the shift to later-eluting vesicles observed when POPC SUVs are used (data not shown). Since the POPC–LPC SUVs are similar in size to POPC SUVs, this indicates that the GM_1 incorporates randomly among all POPC–LPC SUVs. Interestingly, no redistribution of lipid phosphate from the POPC–LPC SUVs was detected at any time, suggesting that LPC spontaneous transfer to GM_1 micelles is negligible under our experimental conditions.

DISCUSSION

Previous studies of the spontaneous transfer of gangliosides from their micelles to phospholipid vesicles were limited to LUVs partly because no reliable technology existed for separating the micelles and SUVs. However, the advent of better molecular sieving gels with more discriminating high molecular weight fractionation ranges has alleviated such problems and permitted ganglioside incorporation to be studied with phospholipid vesicles of differing size. As a result, we now know that the spontaneous uptake of ganglioside is quite sensitive to vesicle size. Size is important because it can directly affect collisional frequency between GM_1 monomers and vesicles as well as the packing of individual lipid molecules comprising the vesicle's surface. The relative contribution of these two parameters to the results of this study as well as possible implications for other studies in which exogenous gangliosides have been incubated with cells are considered below.

To estimate and compare the diffusion-controlled collisional rate constants between ganglioside monomers and either LUVs or SUVs, we used the theory of Schmoluchowski (1917). For uncharged spherical particles, the rate constant for a bimolecular collision can be expressed in terms of the collision complex radius and the diffusion coefficients of the reacting species, where N_A is Avagadro's number. Because the vesicles are very large compared to GM_1 monomers, the collision complex radius is dominated by the vesicle radius, whereas the diffusional term is dominated by the lipid monomer's diffusion coefficient [e.g., Elamrani and Blume (1982)]:

$$k_{coll} = (4N_A/1000)D_{GM1}r_v$$

Accordingly, when lipid concentrations are corrected for differences in the number of vesicles per micromole of phospholipid and the available outer surface area per vesicle (Silversmith & Nelsestuen, 1986), ganglioside monomers will collide with SUVs about 8 times more frequently than with LUVs. If collisions between GM_1 monomers and SUVs are equally effective in promoting uptake as those between GM_1 monomers and LUVs, then the increased frequency in collisions is sufficient to explain the experimentally observed differences. However, as shown in the RESULTS, GM_1's preference for SUVs is not limited to SUV–LUV mixtures but is also observed within SUV populations. The size variation of vesicles comprising a population of SUVs is insufficient to affect their collisional frequency enough to explain GM_1's preference for the smaller vesicles of SUV populations.

Another parameter that could account for GM_1's preference to incorporate into the smaller vesicles of an SUV population is the curvature-induced change in vesicle surface structure. In fact, because the curvature of the inner and outer monolayers of SUVs differs in both magnitude and sign, distinct geometric constraints are placed on the lipid molecules comprising each half of the bilayer. Formation of SUVs requires that the geometric constraints be satisfied in a manner suited to the molecular architecture and hydration properties of the component lipids. Such effects are clearly evident in SUVs whether they are comprised of POPC or of LPC–POPC mixtures.

In SUVs, curvature-induced constraints have been studied theoretically (Dill & Flory, 1981) and experimentally by a variety of techniques. The motional properties and surface area available for the lipid polar headgroups (Kroon et al., 1976; Gaber & Peticolas, 1977; Huang & Mason, 1978; Eigenberg & Chan, 1980) and the fatty acyl packing are not the same in each half of SUVs (Sheetz & Chan, 1972, Longmuir & Dalquist, 1976; Chrzeszczyk et al., 1977; Gaber & Peticolas, 1977; Schuh et al., 1982) and differ from those encountered in planar bilayer membranes (e.g., LUVs) or in SUVs comprised of LPC–POPC (1:3) mixtures (Kumar et al., 1989). As a result, important interfacial physical properties like surface pressure are different in SUVs and LUVs. The surface pressure in the outer monolayer of a 25-nm-diameter DMPC SUV is 21 dyn/cm, of a 40-nm-diameter vesicle is 30 dyn/cm, and of a 75-nm-diameter vesicle is 38 dyn/cm, and the pressure reaches 46 dyn/cm for a 200-nm-diameter DMPC LUV (MacDonald, 1988; Schindler, 1980). Also, since the phospholipids in the inner monolayer of SUVs are known to be packed tighter, they would be expected to have a higher surface pressure than in LUVs. Thus, there is a surface pressure differential across the bilayer in diacyl-PC SUVs that diminishes as vesicles increase in size. Presumably, there is no surface pressure differential across LPC–POPC SUVs because the extreme curvature is accommodated by "wedging" the LPC asymmetrically into each half of the bilayer, which concomitantly restricts the headgroup motion of POPC in the outer bilayer leaflet (Kumar et al., 1989). The presence of a transmembrane differential in surface pressure bestows many unique properties on diacyl-PC SUVs (Mason & Huang, 1978; Lichtenberg et al., 1981; Liu & Huang, 1989) including making insertion of an amphiphilic lipid like ganglioside GM_1 energetically favored with diacyl-PC SUVs compared to

diacyl-PC LUVs or LPC–POPC SUVs. In fact, membrane surface pressure can account for differential activities of many membrane-penetrating molecules including lipids, proteins, and certain pharmacologic agents [e.g., MacDonald and MacDonald (1988)].

Implications. Our data suggest that the rate of GM_1 transfer from micelles to PC vesicles is sensitive to compositionally-induced changes in "acceptor" membrane packing (e.g., POPC vs POPC–LPC SUVs). While other researchers have noted that temperature-induced changes in the lamellar phase state of acceptor membranes can affect spontaneous lipid transfer rates [e.g., Nichols and Pagano (1981)] compositionally-driven changes, which are likely to be of physiological importance in eukaryotes, have received less attention. Determining whether compositionally-induced changes in acceptor membranes can become rate-limiting will require appropriately fast, kinetic approaches. Indeed, on the basis of fluorescent measurements of temperature-induced lamellar phase changes, Masserini and Freire (1987) have argued that the physical state of the acceptor membrane is the rate-limiting step for the transfer of a fluorescent GM_1 derivative from its micelles to DPPC LUVs.

The low ganglioside concentration used in these studies is physiologically relevant because, under nonpathological conditions, gangliosides are minor components in the plasma membranes of cells (Curatolo, 1987b; Ledeen, 1984). More importantly, the findings reported here provide potential insight into earlier conflicting reports describing the response of cultured cells to exogenously-added gangliosides and the molecular nature of exogenous ganglioside association with cellular plasma membranes. The basic controversy centered over whether exogenously-added gangliosides integrate into plasma membranes and become internalized and metabolized or whether they attach to trypsin-sensitive membrane components and are neither internalized nor metabolized by the cells [for reviews, see Thompson and Brown (1988) and Brown (1990)]. In order to explain the conflicting findings, various experimental conditions were studied. Differences in cell density and/or metabolic state, as well as the presence or absence of serum proteins or other lipids in the cell culture medium, all appear to affect the incorporation of exogenous gangliosides (Fishman et al., 1978; Spiegel et al., 1984; Facci et al., 1984; Sonderfeld et al., 1985; Giglioni et al., 1990).

On the basis of our findings, it appears equally plausible that other surface-related factors warrant consideration. For instance, the plasma membrane surfaces of various cell types may possess regions that differ in their lipid packing and accelerate ganglioside uptake. Membrane regions that are evaginated and possess high curvature, such as microvilli or other microevaginations, would be possible candidates. If the cells lack such regions, then incorporation of gangliosides into the cells membrane may slow because the gangliosides would persist in the micellar state for longer periods. Alternatively, certain cells may shed small membrane vesicles into the medium which act as sinks for arriving gangliosides and prevent them from reaching the plasma membrane surface. In fact, certain cells do form small membrane blebs that are shed into the culture medium [e.g., Beaudoin and Grondin (1991)]. Either of these mechanisms could explain earlier conflicting reports regarding the incorporation of exogenously-added gangliosides into cultured cells. Of course, membrane curvature per se need not be the only way for cells to regulate ganglioside uptake. Certain proteins, residing within (Tiemeyer et al., 1989) or acting upon the membrane surface (e.g., Brown et al., 1990), may facilitate ganglioside uptake by generating the required environment at specific sites within membranes. Determining which of these mechanisms predominates in vivo will require further study.

ACKNOWLEDGMENT

We thank Warren Erdahl and Kari Jarvis for their assistance in purifying the tritiated ganglioside, Wayne Anderson for preparing the freeze-fracture electron micrographs, Carmen Perleberg and Kerry Ruck for secretarial services, and Cores A, E, and G of USPHS PPG HL08214 for drawing the figures and for the use of the EM and HPLC equipment, respectively.

REFERENCES

Ando, S., Waki, H., & Kon, K. (1987) *J. Chromatogr. 405*, 125–134.
Barenholz, Y., Gibbes, D., Litman, B., Goll, J., Thompson, T. E., & Carlson, F. D. (1977) *Biochemistry 16*, 2806–2810.
Beaudoin, A. R., & Grondin, G. (1991) *Biochim. Biophys. Acta 1071*, 203–219.
Brown, R. E. (1990) in *Subcellular Biochemistry: Intracellular Transfer of Lipid Molecules* (Hilderson, H. J., Ed.) Vol. 16, pp 333–363, Plenum Press, New York.
Brown, R. E., & Thompson, T. E. (1987) *Biochemistry 26*, 5454–5460.
Brown, R. E., & Hyland, K. J. (1992) *Biophys. J. 61*, A493.
Brown, R. E., Sugar, I. P., & Thompson, T. E. (1985) *Biochemistry 24*, 4082–4091.
Brown, R. E., Jarvis, K. L., & Hyland, K. J. (1990) *Biochim. Biophys. Acta 1044*, 77–83.
Cantu, L., Corti, M., Sonnino, S., & Tettamanti, G. (1986) *Chem. Phys. Lipids 41*, 315–328.
Chapman, C. J., Erdahl, W. L., Taylor, R. W., & Pfeiffer, D. R. (1990) *Chem. Phys. Lipids 55*, 73–83.
Chrzeszczyk, A., Wishnia, A., & Springer, C. S. (1977) *Biochim. Biophys. Acta 470*, 161–169.
Corti, M., Cantu, L., & Salina, P. (1991) *Adv. Colloid Interface Sci. 36*, 153–171.
Curatolo, W. (1987a) *Biochim. Biophys. Acta 906*, 111–136.
Curatolo, W. (1987b) *Biochim. Biophys. Acta 906*, 137–151.
Dill, K. A., & Flory, P. J. (1981) *Proc. Natl. Acad. Sci. U.S.A. 78*, 676–680.
Eigenberg, K. E., & Chan, S. I. (1980) *Biochim. Biophys. Acta 599*, 330–335.
Elamrani, K., & Blume, A. (1982) *Biochemistry 21*, 521–526.
Facci, L., Leon, A., Toffano, G., Sonnino, S., Ghidoni, R., & Tettamanti, G. (1984) *J. Neurochem. 42*, 299–305.
Felgner, P. L., Freire, E., Barenholz, Y., & Thompson, T. E. (1981) *Biochemistry 20*, 2168–2172.
Felgner, P. L., Thompson, T. E., Barenholz, Y., & Lichtenberg, D. (1983) *Biochemistry 22*, 1670–1674.
Fishman, P. H., Bradley, R. M., Moss, J., & Manganiello, V. C. (1978) *J. Lipid Res. 19*, 77–81.
Gaber, B. P., & Peticolas, W. L. (1977) *Biochim. Biophys. Acta 465*, 260–274.
Giglioni, A., Chigorno, V., Pitto, M., Valsecchi, M., Palestini, P., & Ghidoni, R. (1990) *Chem. Phys. Lipids 55*, 207–213.
Hakomori, S. (1990) *J. Biol. Chem. 265*, 18713–18716.
Hannun, Y. A., & Bell, R. M. (1989) *Science 243*, 500–507.
Harris, P. L., & Thornton, E. R. (1978) *J. Am. Chem. Soc. 100*, 6738–6745.
Huang, C., & Mason, J. T. (1978) *Proc. Natl. Acad. Sci. U.S.A. 75*, 308–310.
Jackson, M., Schmidt, C. F., Lichtenberg, D., Litman, B. J., & Albert, A. D. (1982) *Biochemistry 21*, 4576–4582.
Karlsson, K. (1989) *Annu. Rev. Biochem. 58*, 309–350.
Kroon, P. A., Kainosho, M., & Chan, S. I. (1976) *Biochim. Biophys. Acta 433*, 282–283.
Kumar, V. V., Malewicz, B., & Baumann, W. J. (1989) *Biophys. J. 55*, 789–792.

Kundu, S. (1981) *Methods Enzymol. 72*, 185–204.
Ledeen, R. W. (1984) *J. Neurosci. Res. 12*, 147–159.
Lichtenberg, D., & Barenholz, Y. (1988) *Methods Biochem. Anal. 33*, 337–462.
Lichtenberg, D., Freire, E., Schmidt, C. F., Barenholz, Y., Felgner, P. L., & Thompson, T. E. (1981) *Biochemistry 20*, 3462–3467.
Liu, D., & Huang, L. (1989) *Biochemistry 28*, 7700–7707.
Longmuir, K. J., & Dahlquist, F. W. (1976) *Proc. Natl. Acad. Sci. U.S.A. 73*, 2716–2719.
MacDonald, R. C. (1988) in *Molecular Mechanisms of Membrane Fusion* (Ohki, S. W., Doyle, D., Flanagan, T. D., Hui, S. W., & Mayhew, E., Eds.) pp 101–112, Plenum, New York.
MacDonald, R. C., & MacDonald, R. I. (1988) *J. Biol. Chem. 263*, 10052–10055.
Mason, J. T., & Huang, C. (1978) *Ann. N.Y. Acad. Sci. 308*, 29–49.
Masserini, M., & Freire, E. (1987) *Biochemistry 26*, 237–242.
Mayer, L. D., Hope, M. J., & Cullis, P. R. (1986) *Biochim. Biophys. Acta 858*, 161–168.
Naoi, M., Lee, Y. C., & Roseman, S. (1974) *Anal. Biochem. 58*, 571–577.
Nozaki, Y., Lasic, D. D., Tanford, C., & Reynolds, J. A. (1982) *Science 217*, 366–367.
Reynolds, J. A., Nozaki, Y., & Tanford, C. (1983) *Anal. Biochem. 130*, 471–474.
Rouser, G., Fleischer, S., & Yamamoto, A. (1970) *Lipids 5*, 494–496.
Schindler, H. (1979) *Biochim. Biophys. Acta 555*, 316–336.
Schlenk, H., & Gellerman, J. L., (1960) *Anal. Chem. 32*, 1412–1414.
Schuh, J. R., Banerjee, U., Muller, L., & Chan, S. I. (1982) *Biochim. Biophys. Acta 687*, 219–225.
Sheetz, M. P., & Chan, S. I. (1976) *Biochemistry 11*, 4573–4581.
Silversmith, R. E., & Nelsestuen, G. L. (1986) *Biochemistry 25*, 7717–7725.
Sloan-Stanley, G. H. (1967) *Biochem. J. 104*, 293–295.
Smoluchowski, M. (1917) *Z. Phys. Chem., Stoechiom. Verwandtschaftsl. 92*, 129–168.
Sonderfeld, S., Conzelmann, E., Schwarzmann, G., Burg, J., Hinrichs, U., & Sandhoff, K. (1985) *Eur. J. Biochem. 149*, 247–255.
Spiegel, S., Schlessinger, J., & Fishman, P. H. (1984) *J. Cell Biol. 99*, 699–704.
Thompson, T. E., & Brown, R. E. (1988) in *New Trends in Ganglioside Research: Neurochemical and Neuroregenerative Aspects* (Ledeen, R. W., Hogan, E. L., Tettamanti, G., Yates, A. J., & Yu, R. K., Eds.) Fidia Research Series, Vol. 14, pp 65–78, Liviana Press, Padova, Italy.
Tiemeyer, M., Yasuda, Y., & Schnaar, R. L. (1989) *J. Biol. Chem. 264*, 1671–1681.
van Venetie, R., Leunissen-Bijvelt, J., Verkleij, A. J., & Ververgaert, P. H. J. Th. (1980) *J. Microsc. 118*, 401–408.
Williams, M. A., & McCluer, R. H. (1980) *J. Neurochem. 35*, 266–269.